

# IMPACT OF DEPOSITION AND DIAGENESIS ON QUALITY OF SANDSTONE RESERVOIRS: A CASE STUDY IN CUU LONG BASIN, OFFSHORE VIETNAM

**Nguyen Trung Son**

Vietnam Petroleum Institute

Email: sonnt@vpi.pvn.vn

<https://doi.org/10.47800/PVJ.2022.06-02>

## Summary

Sandstone reservoirs are major reservoirs in siliciclastic rocks worldwide. A good understanding of the development of internal rock properties is, therefore, extremely important, especially in terms of porosity and permeability (which indicate reservoir storage and flow capacity), which are controlled by mineral compositions, rock textures, and diagenetic processes. This paper studied formations E and F in three wells in the Cuu Long basin to better define the impacts of not only depositional characters but also diagenetic overprints on porosity and permeability (poroperm). Core samples were analysed via thin section observations, scanning electron microscopy (SEM), X-ray diffraction (XRD) observations, capillary pressure (P<sub>c</sub>) and helium porosity - permeability measurements together with petrophysical evaluation.

Formation E was deposited in a fluvial - lacustrine environment that is characterised by claystone/shale interbedded with sandstone, with reduced depositional permeability in finer-grained intervals. XRD and SEM analyses indicate rock quality in the sandstone reservoirs was influenced by a variety of authigenic minerals, such as carbonate cements, quartz overgrowths, zeolites, and laumontite clays, which all tend to reduce poroperm. Whereas, formation F was deposited in a higher energy setting. This was mostly a braided channel environment indicated by a blocky shape in the wireline across the sandy interval and typically good primary porosity and permeability. In formation F, the reservoir quality is strongly controlled by diagenetic evolution. Pore throats in the E and F sandstones are reduced in size by intense compaction and a combination of pore-filling minerals including calcite cements, authigenic clays, and quartz overgrowths, leading to a negative relationship with poroperm. However, this negative relationship is not as clear in the formation E.

**Key words:** Formations E and F, depositional environment, diagenetic process, petrography, porosity and permeability.

## 1. Introduction

This study discusses deposition, diagenesis and quality of sandstone reservoirs using a case study in the Cuu Long basin, offshore Vietnam (Figure 1). By creating a better understanding of the controls in the development of poroperm and the diagenetic evolution of formations E and F, the study aims to establish key factors that influence reservoir quality. The work is based on the integration of rock properties with petrographic analysis (thin section petrography, XRD, SEM analyses, capillary pressure (P<sub>c</sub>), and petrophysical evaluation. Results will help to

better constrain the depositional environment and diagenetic processes in the study area.

## 2. Geological setting

The Cuu Long basin is a rift basin that experienced two main deformational events: (i) trans-tensional rifting from the Eocene to Middle - Early Oligocene (40 - 31 Ma), followed by (ii) a transpression from the Middle - Early Oligocene to the Middle - Late Oligocene (31 - 25 Ma). This created three major tectonic styles, namely: (i) rifting-related normal faulting from the Early Eocene to Middle - Early Oligocene, (ii) compression-related reverse faults and folds generated from the Middle - Early Oligocene to Middle - Late Oligocene, and (iii) thermal sagging from the Middle - Late Oligocene to the present, when the ba-



Date of receipt: 25/2/2022. Date of review and editing: 25/2 - 28/4/2022.

Date of approval: 27/6/2022.

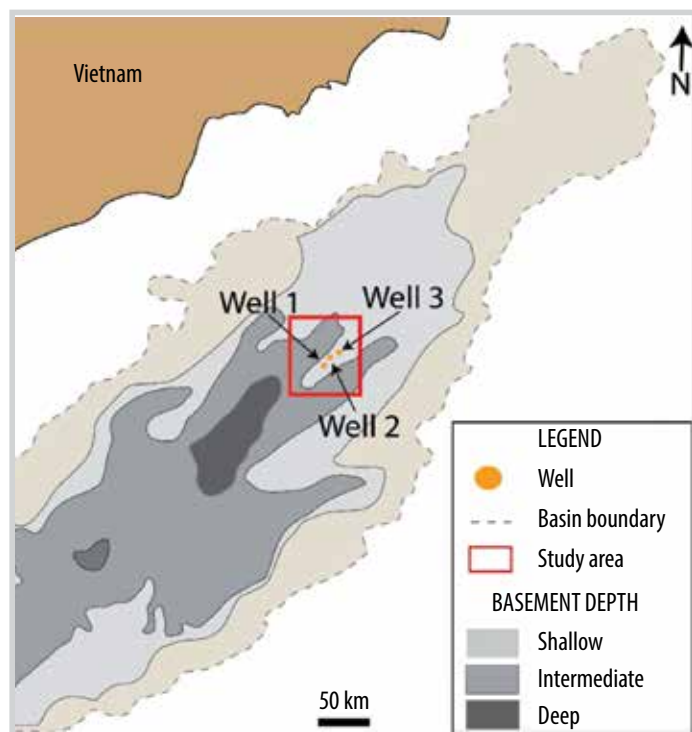


Figure 1. Overview of the study area (modified from Morley et al. [1]).

Period	Formation	Lithology	Seismic sequence	Description	Depositional environment	Tectonic regime
Pliocene-Quaternary	Bien Dong	[Yellow with green speckles]	A	Coarse grained, unconsolidated sand, shale, interbedded with carbonate and coal layers	Marine	Thermal Sag
Miocene	Late Dong Nai	[Yellow with green speckles]	B3	Coarse to fine grained sand, coal, minor carbonate layers	Coastal plain, shallow marine	
	Middle Con Son	[Yellow with green speckles]	B2	Sand, shale, coal, minor carbonate layers	Fluvial, marginal marine	
Oligocene	Early Bach Ho	[Yellow with green speckles]	B1.2	Shale dominant with interbedded sand	Swamp, alluvial-lacustrine	Compression
	Late Tra Tan	[Yellow with green speckles]	B1.1	Interbedded sand, silt, and shale; basalt and tuff basalt in places	Swamp-lacustrine	
Eocene	Late Tra Cu	[Yellow with green speckles]	E	Shale, silt and sand, with thin coal and marl layers	Alluvial to swamp-lacustrine	Rifting
	Early Ca Coi	[Yellow with green speckles]	F	Conglomerate and sandstone with thin shale layers	Proluvial-alluvial	
Pre-Tertiary		[Red with white fractures]		Weathered and fractured granitoids and metamorphic rocks		

Figure 2. The stratigraphic column of the study area, focusing on formations E and F marked by a blue rectangle (modified from Morley et al [1] and W.J. Schmitt [4]).

sin is fully filled by sediment without major faulting [1] which were affected by two main fault systems, NE-SW and NW-SE, of the Cuu Long basin [2]. Accommodation space in the Cuu Long basin is completely filled with Tertiary sediments, of which the Eocene F sequence is the oldest in the basin, followed by the Eocene - Oligocene E sequence, which includes sequences E, C and D. The Eocene succession is characterised by the Tra Cu and Ca Coi formations, which embrace sequences E and F [3]. Sandstones E and F, which are the focus of this study, were deposited in the Early - Middle Eocene (F) and the Late Eocene to Early Oligocene (E) (Figure 2).

### 3. Methodology

For the first time, the results of several sets of analysis across the three wells are integrated and combined in a multi-well synthesis. The aim is to better define controls on porosity and permeability in terms of not only depositional characters but also diagenetic overprints. Diagenetic intensity is estimated vertically and horizontally (among the wells) based on integration of reservoir properties. Core photos, core analyses and the results of the petrographic study are integrated with helium-based porosity-permeability measured by routine core analysis (RCA) and capillary pressure. Thin sections, SEM log shape and core data from all wells are proved useful in defining various depositional environments in the study area. Depositional environments are cross-plotted against each other to better identify lithological variability and its tie to poroperm quality.

### 4. Results

#### 4.1. Core interpretation

Lacustrine shoreface/deltaic sandflat: Fine-grained sandstone is typical of this facies grouping. The primary structure is low-angle bedding and indeterminate lamination (Figure 3).

Channel/channel abandonment: These fining-upward sandy reservoir-quality units include mud rip-up clasts and some coarse grains at their bases that then pass up into cross-bedded units with muddy tops (Figure 4).

Overbank: These are very fine-grained sediments formed from mudstones and very fine siltstones that

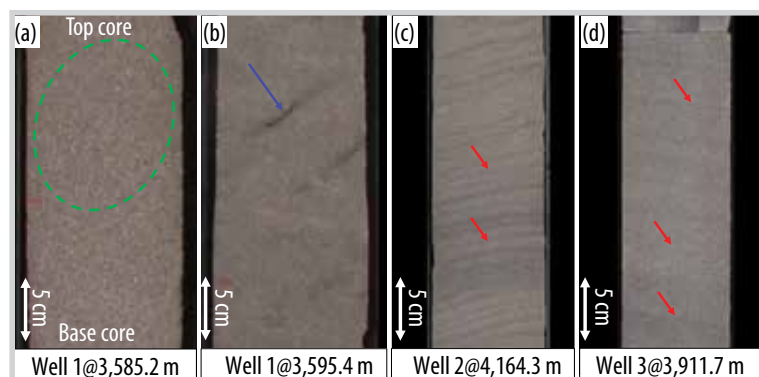


**Figure 3.** (a) Massive medium sandstone with a mottled texture (green oval) indicating extensive bioturbation, (b) Fine sandstone including plant fragments (blue arrow), (c) Low-angle lamination (red arrow) with fine-grained sand interlaminated with thin shales, and (d) Indeterminate lamination (red arrow) with fine grain size.

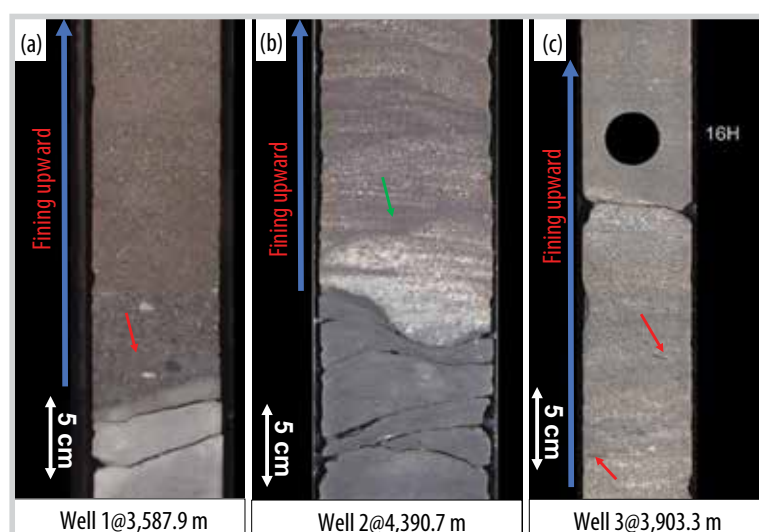


**Figure 4.** (a) Fining-upward sandstones include very coarse grains and granules; mudstone clasts occur within some beds (red arrow), (b) Primary sedimentary structures are dominated by planar cross-bedding (green arrow) with fining-upward trends and erosional bases, exaggerated by compactional loading, (c) The fining-upward trend with the only fossil material is observed within these facies being small plant fragments (red arrow).

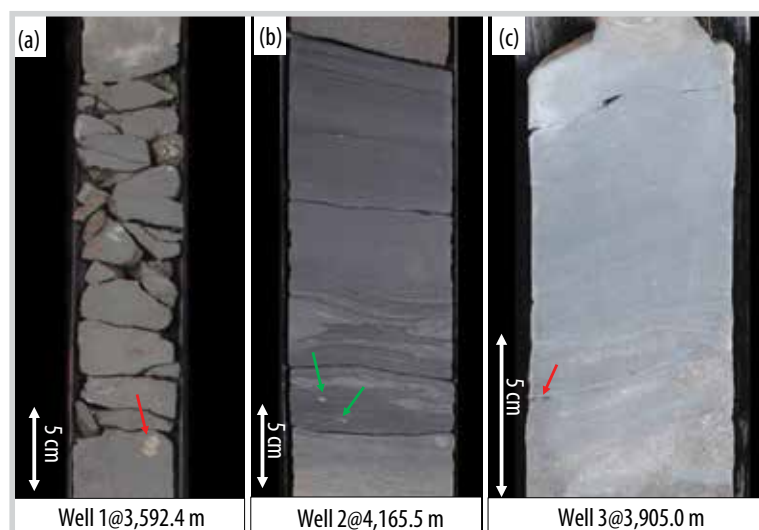


**Figure 5.** (a) Mudstones and very fine siltstones include occasional nodular pyrite (arrow) and sand-filled burrows (at the top) in well 1, (b) Mudstones and some nodular pyrite (arrow) in well 2, (c) Very fine siltstone includes a calcite-cement mud clast (arrow).

include some sandstone-filled burrows. There are some pyrite nodules and calcite-cemented mud clasts in several intervals (Figure 5).

**Braided fluvial:** These sandstones range in grain size from very fine (lower) to coarse (middle). The thickness of individual beds varies from about 10 cm to 1.65 m. The sandstones are usually composed of mud rip-up clasts, very coarse grains, granules and pebbles which are most common within bed bases (Figure 6).

**Depositional environment interpretation:** In general, the textural features and framework-grain compositions (lithic-arkoses and arkoses, Figure 9) of the E sandstone indicate that the sediments were transported over a distance not too far from the source, and that during deposition the sands were frequently affected by periods of at least moderate current activity (sand deposition) alternating with periods of quiescence (clay deposition). In combination with the palynology, it suggests that the sediments were deposited in a mostly lacustrine and fluvial environment [5].

Textural features and framework-grain compositions of the F sandstone indicate that the sediments were transported not too far from the source and that this sandstone was frequently subjected by high energy flows in a braided fluvial setting.

#### 4.2. Petrophysical analysis

Helium analytical results on core plugs from formations E and F show a wide range of porosity and permeability. In formation E, porosity varies from 2 to 16% ( $\Phi_{avg.} = 9.7\%$ ) and permeability from 0.001 to 1,000 mD ( $K_{avg.} = 30.8$  mD). The F formation generally shows higher values than the E formation, with porosity ranging from 2 to 18% ( $\Phi_{avg.} = 10.6\%$ ) and permeability from 0.0001 to more than 1,000 mD ( $K_{avg.} = 66.7$  mD). Cross-plots of porosity and permeability show a good correlation in both formations, with linear relationships.

The curvature of capillary pressure curves indicates the rock quality. The examples of formations E and F show more gentle curvatures related to reduced permeability due to the



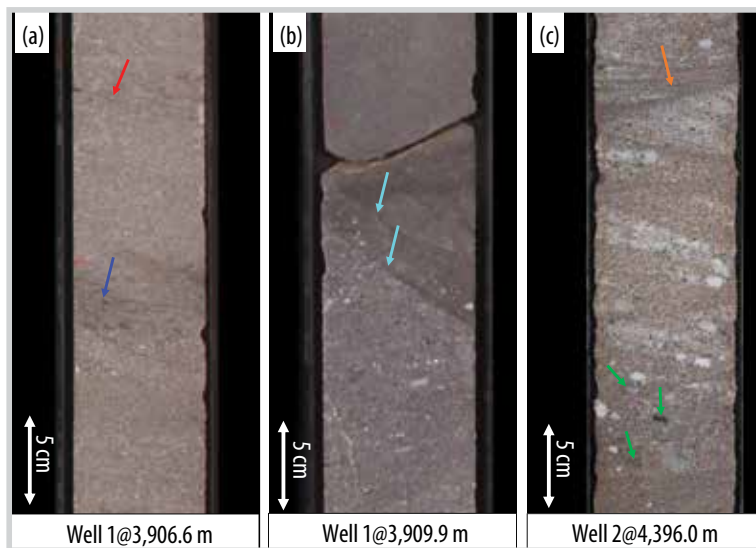


**Figure 6.** (a) The sandstones commonly include mud clasts, very coarse grains, granules and pebbles (blue arrow). Fossil material includes some small plant fragments (red arrow) (b) A sequence of low-angle normal fractures at the contact between coarse and very fine sandstones. Fractures are clay smeared (aqua arrow) (c) The dominant primary sedimentary structure is planar cross-bedding which ranges in dip from horizontal to 45° (orange arrow). Some of the pebbles comprise green basement clasts, which are possibly basalt (green arrow).

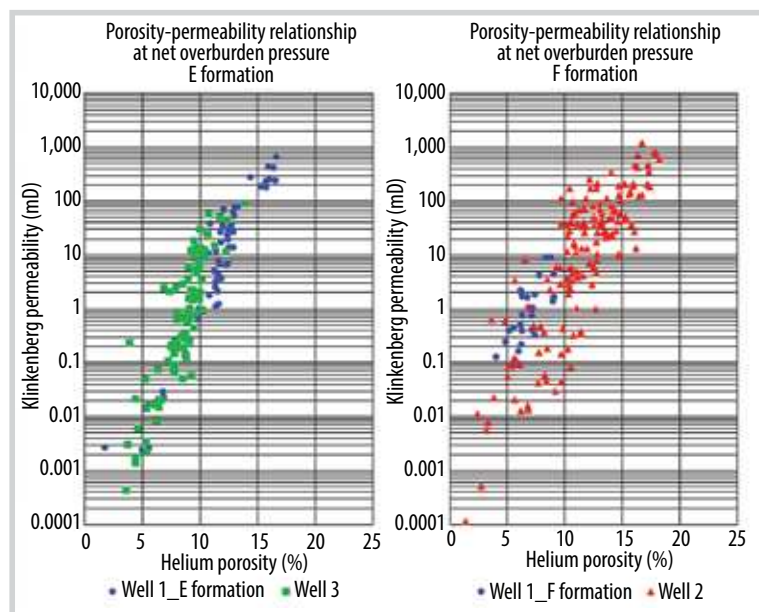


**Figure 7.** Cross-plots illustrating the relationship between porosity and permeability in formations E and F.

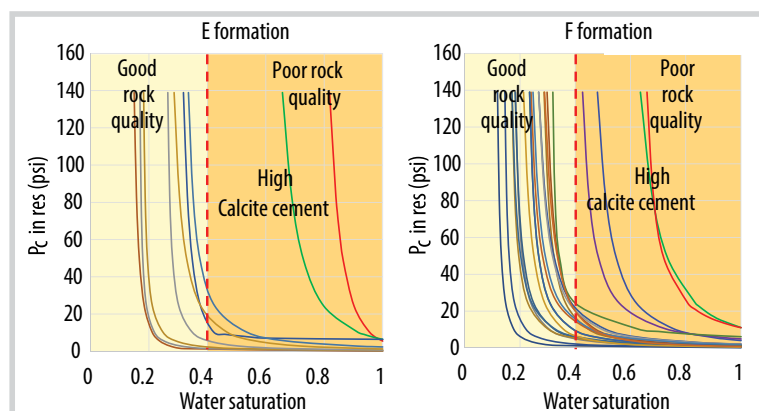


**Figure 8.** The curvature of the capillary pressure curve indicates the rock quality.

impact of calcite cements in the sands. Poorer quality samples show high residual water saturation related to poorer sorting, and finer grain sizes or poorer quality outputs can be related to calcite cements that have a negative impact on poroperm characteristics. The analysis implies that there are relatively high porosity and permeability intervals within the overall lower porosity-permeability of the dominant reservoirs.

### 4.3. Petrographic analysis

#### 4.3.1. Sandstone detrital composition

Petrographic study shows the cored intervals in well 1, well 2 and well 3. The R.L. Folk classification [6] is used to classify sandstones with less than 15% detrital matrix. The Q, F, and R components are: Q = all quartz, except chert; F = feldspar + granitic fragments; and R is all other rock fragments. Most of the samples are arkosic sandstones and lithic arkose sandstones (Figure 9).

#### 4.3.2. Visible porosity

Porosity in the E and F sandstones includes primary intergranular porosity (i.e. the space between grains) and secondary porosity which is mainly related to the dissolution of unstable detrital grains, such as volcanic fragments and feldspars (K-feldspar and plagioclase). The mechanical compaction of this cored interval is moderate, characterised by grain contacts that are mostly point-to-point (blue arrow); some long-axis (green arrow) passing to occasional concavo-convex contacts (yellow arrow).

#### 4.3.3. Mineral framework grains

Whole-rock analysis of samples in the cored intervals shows quartz dominance. Feldspars are the second most abundant component in the sandstones and consist of two types, potassium feldspar (K-F) and plagioclase. Petrography shows that feldspar dissolution has generated secondary porosity, thus enhancing the total porosity.

Well 1\_E sandstone is mainly composed of quartz (average 40%), K-feldspar and plagioclase.

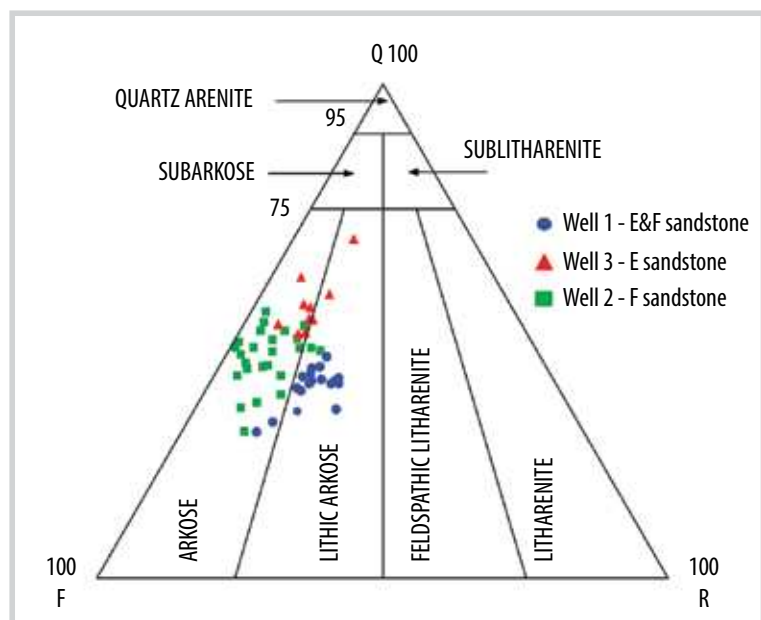


Figure 9. The detrital composition of samples with less than 15% detritals using R.L. Folk's classification [6].

gioclase (average 40%), clay minerals such as mica, laumontite, kaolinite (average 18%); carbonate minerals, calcite, dolomite, and siderite are scarcely present (average 2%) (Figure 11b). In comparison, XRD analysis of samples from well 3 (Figure 11d) has quartz averaging 29% and 38% in their K-F and plagioclase, respectively. This is lower than in well 1, perhaps because the sedimentary source is different. The clay mineral contents in well 3 are higher than in well 1, perhaps because well 3 was further from the sediment source than well 1, or it was deposited under lower overall energy conditions. Carbonate cement content in well 3 (3%) is slightly higher than in well 1 (2%).

Samples of well 1 in the F sandstone mainly consist of quartz (average 54%), K-feldspar and

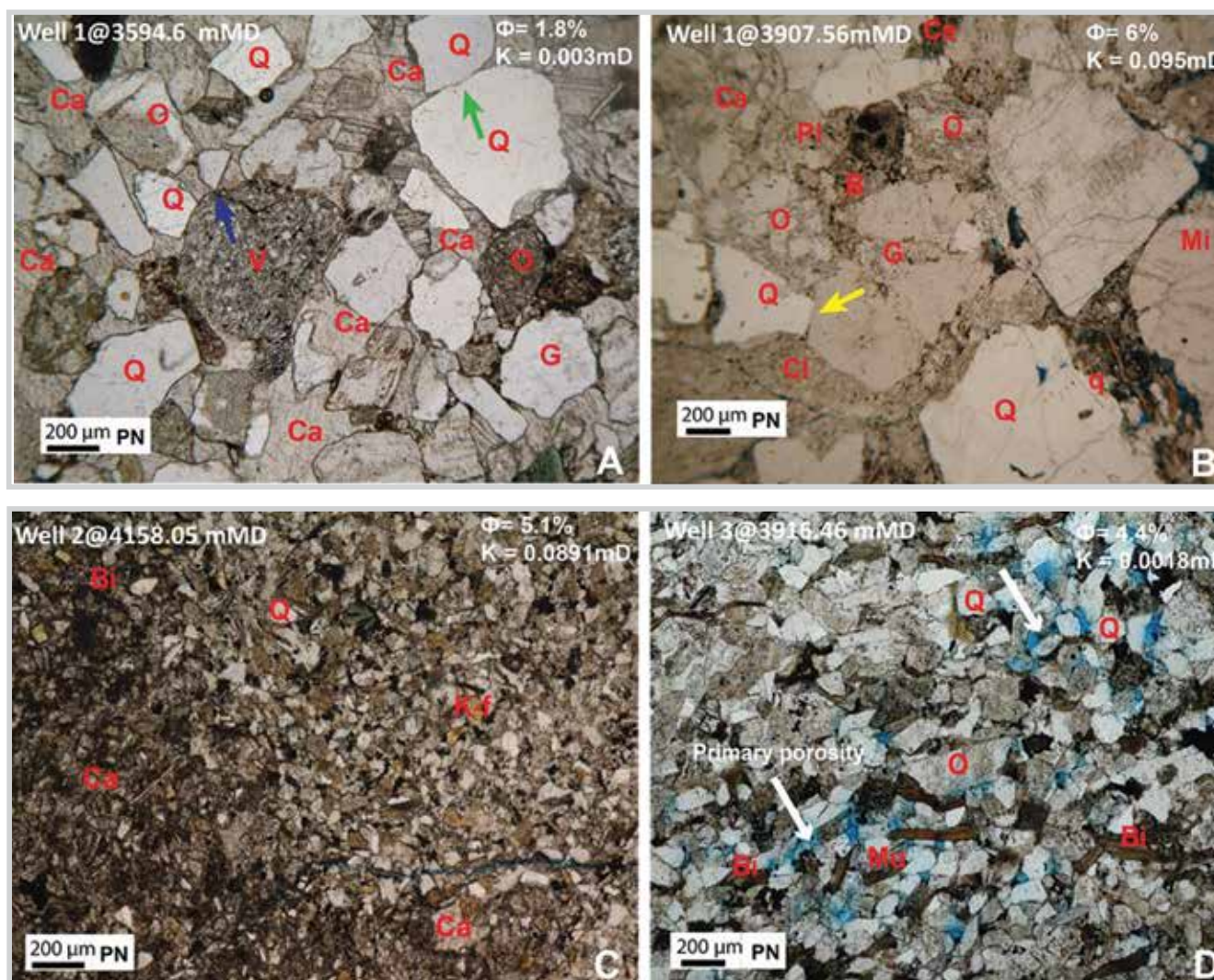


Figure 10. Thin section images of sandstones (pore space is shown in blue; calcite cements (Ca) fill or partly fill intergranular pore spaces. (Q = quartz, q = quartz overgrowths, O = orthoclase, Pl = plagioclase, G = granitic, Bi = volcanic fragments biotite, and Mu = muscovite).

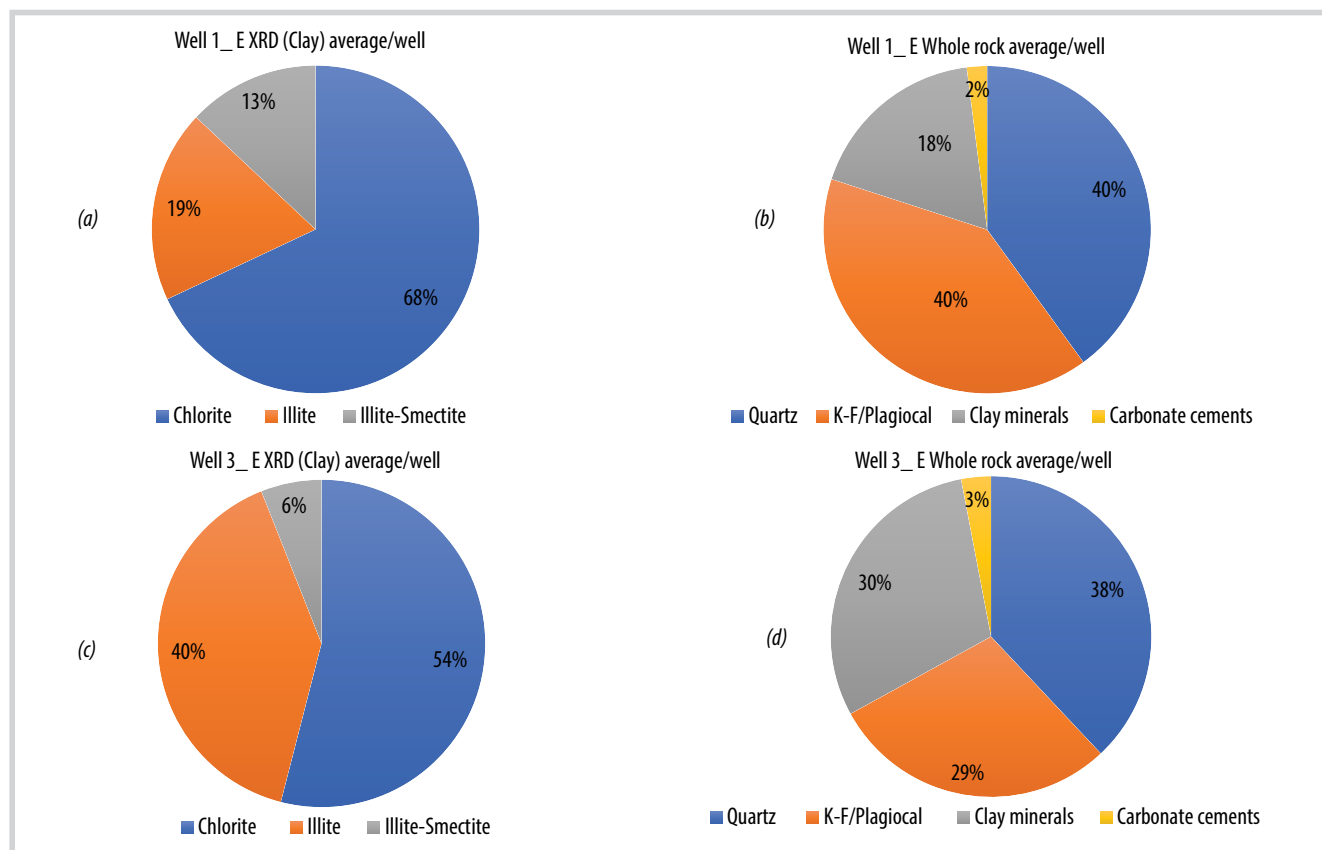


Figure 11. Illustrating the whole rock and XRD results in the E sandstone.

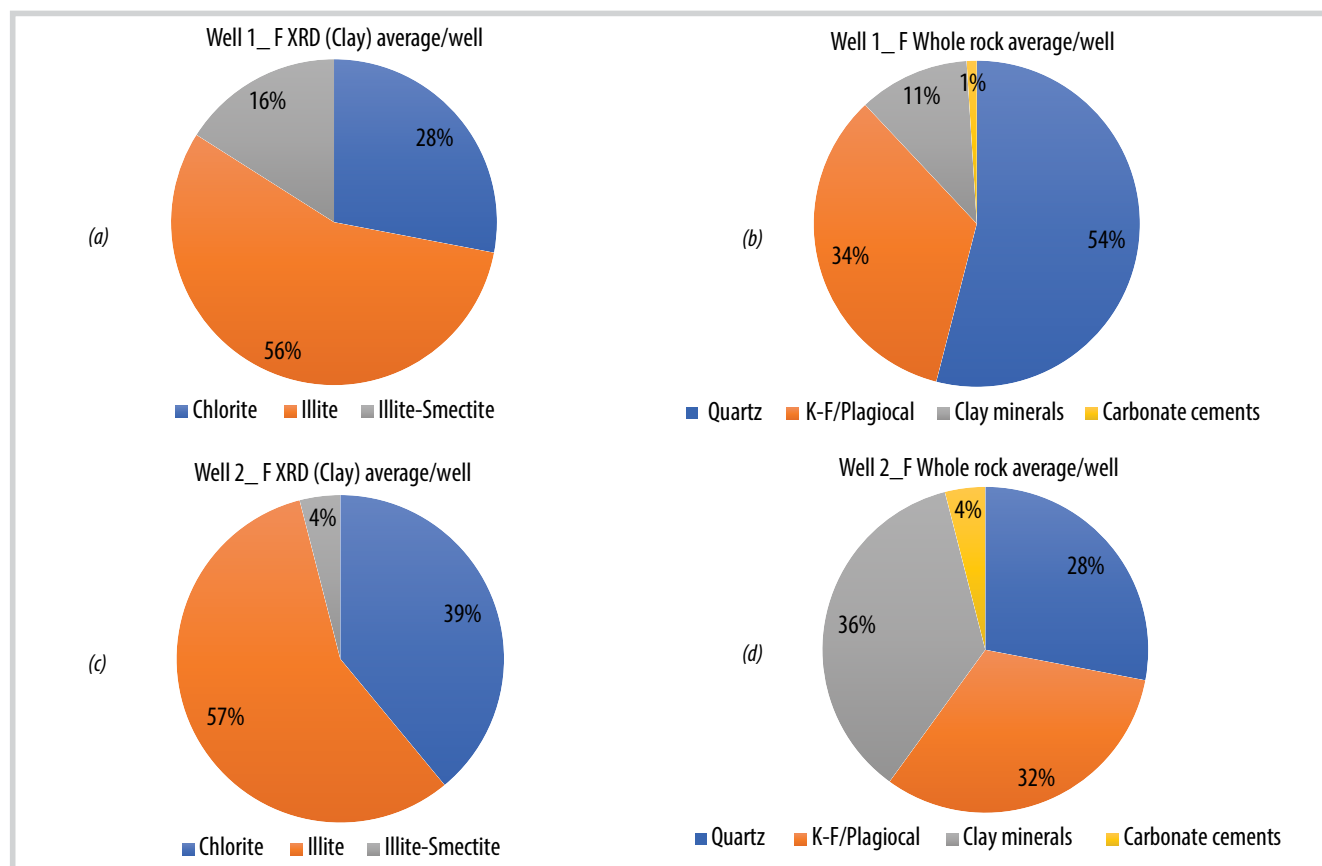


Figure 12. Illustrating the whole rock and XRD results in the F sandstone.



plagioclase (average 34%), other clays such as mica, laumontite, kaolinite (average 18%) and the carbonate minerals, calcite, dolomite and siderite (average 1%) (Figure 12a). In comparison, the F sandstone in well 2 has a quartz average of about 28% and 36% of K-feldspar/plagioclase

(Figure 12d). This is lower than in well 1 and reflected in the petrographic typing of well 1, which is mostly lithic arkose with less feldspar than the arkoses that dominate in well 2 (Figure 9).

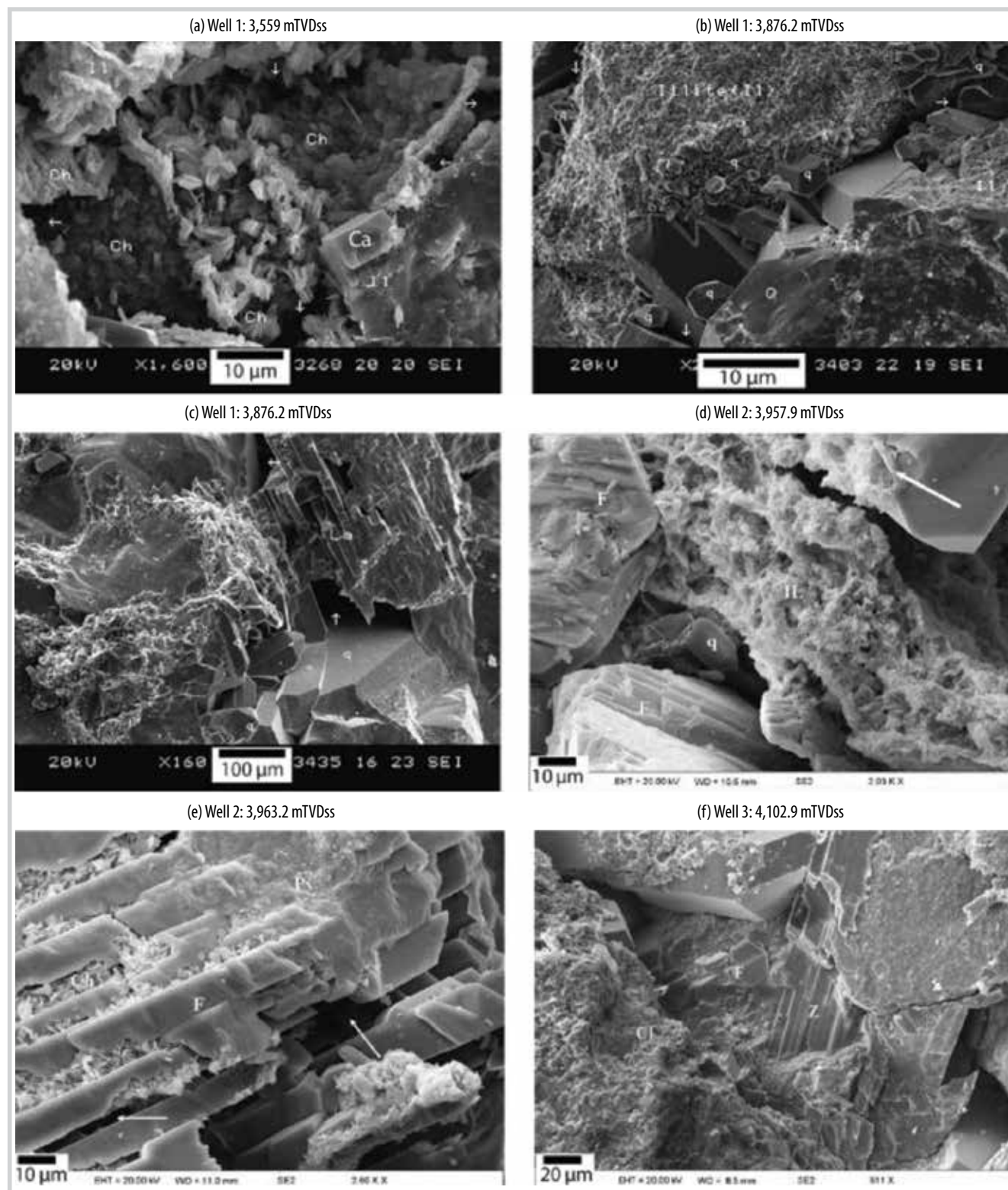
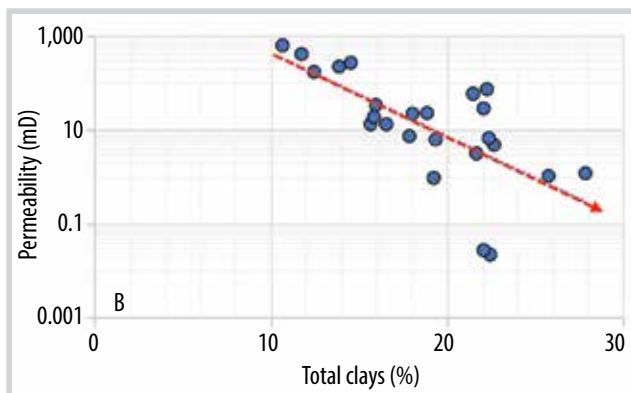
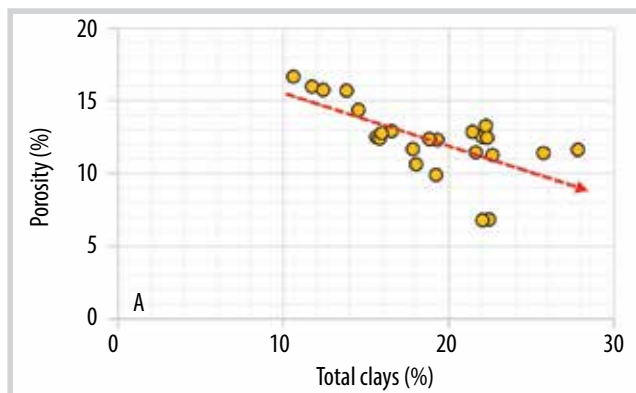


Figure 13. SEM images of samples from all wells in the study area.

Well 1\_E formation



Well 3\_E formation

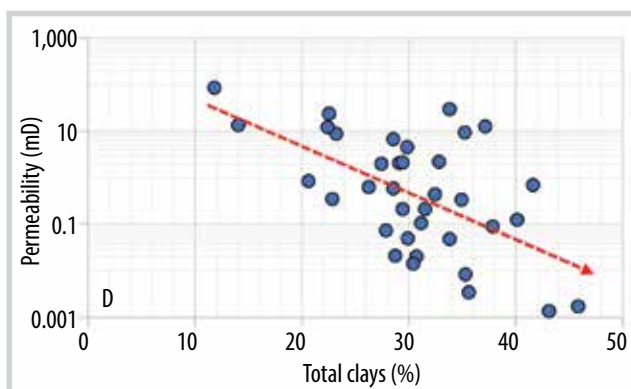
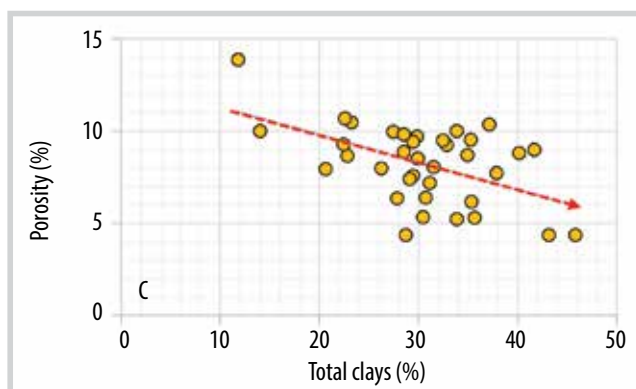
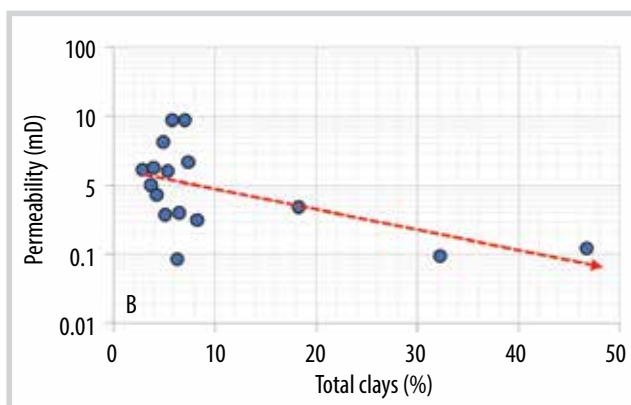
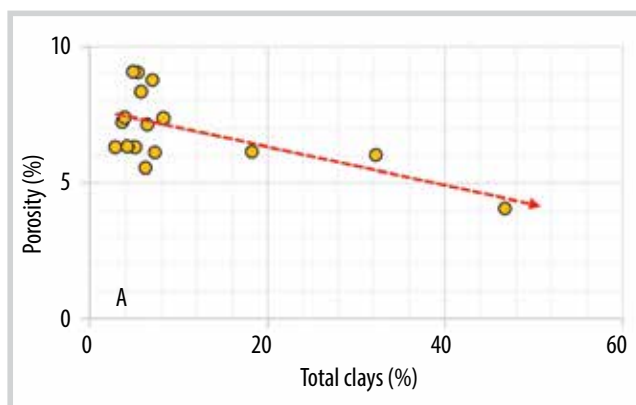


Figure 14. The relationship between permeability and total clays shows a negative trend in formation E.

Well 1\_F formation



Well 2\_F formation

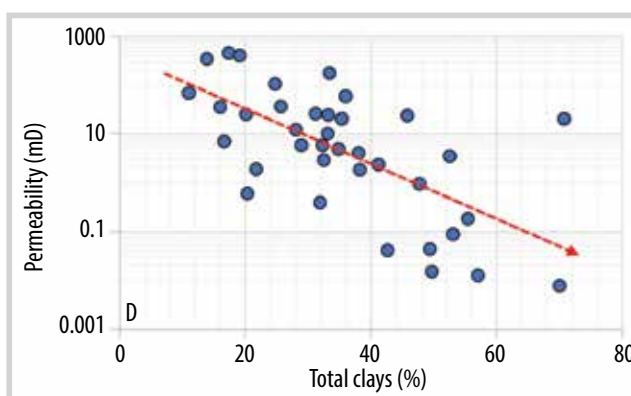
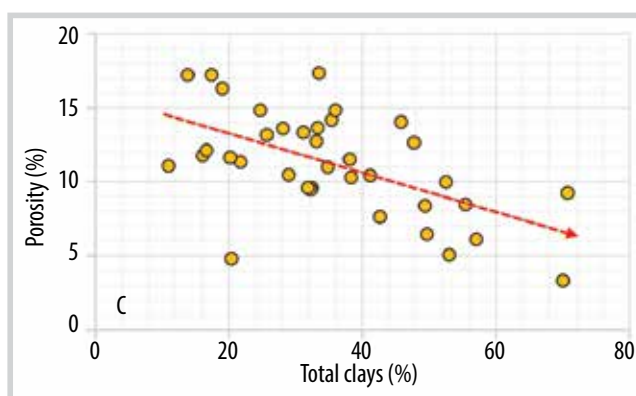


Figure 15. The relationship between permeability and total clay shows a negative trend in formation F.



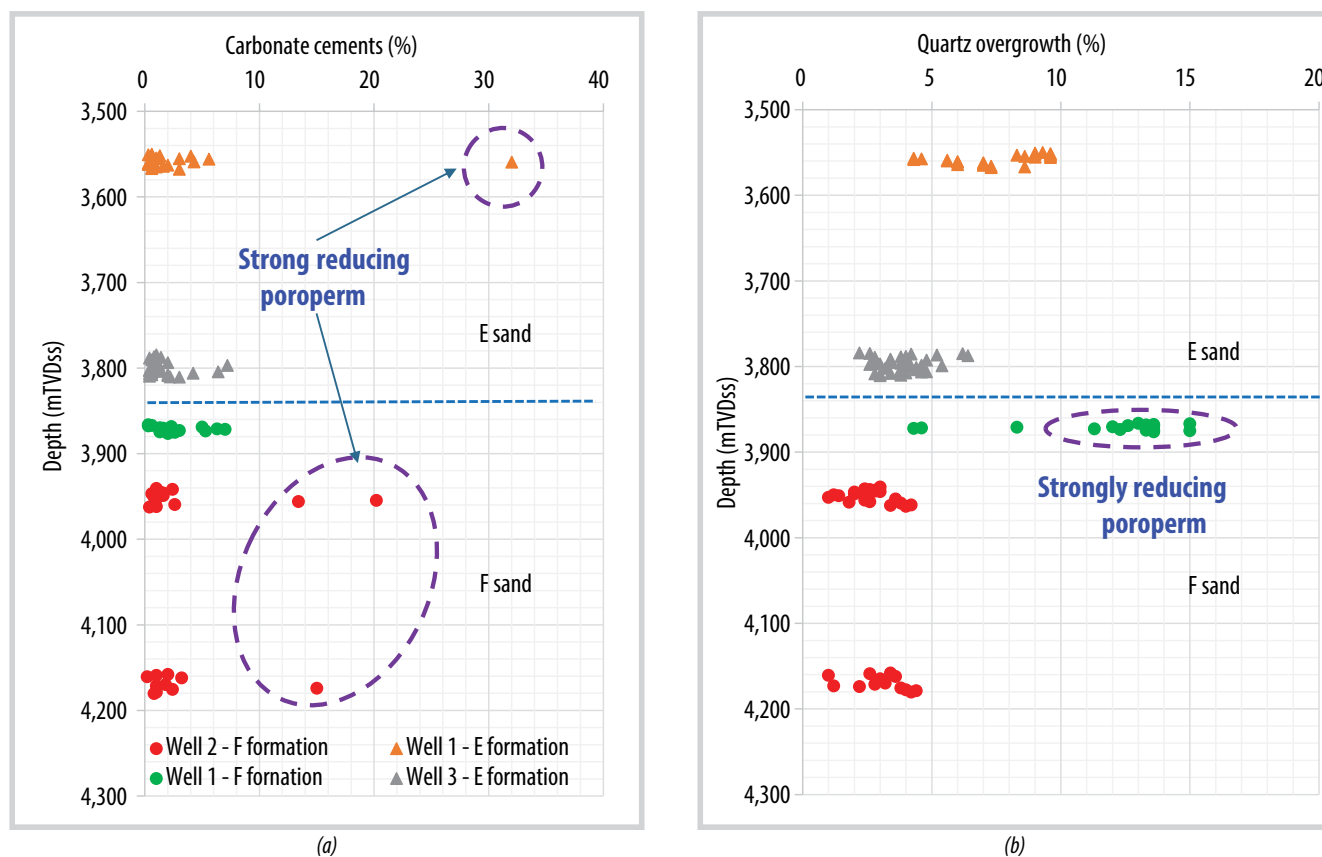


Figure 16. The proportion of carbonate cements and quartz overgrowth distribution.

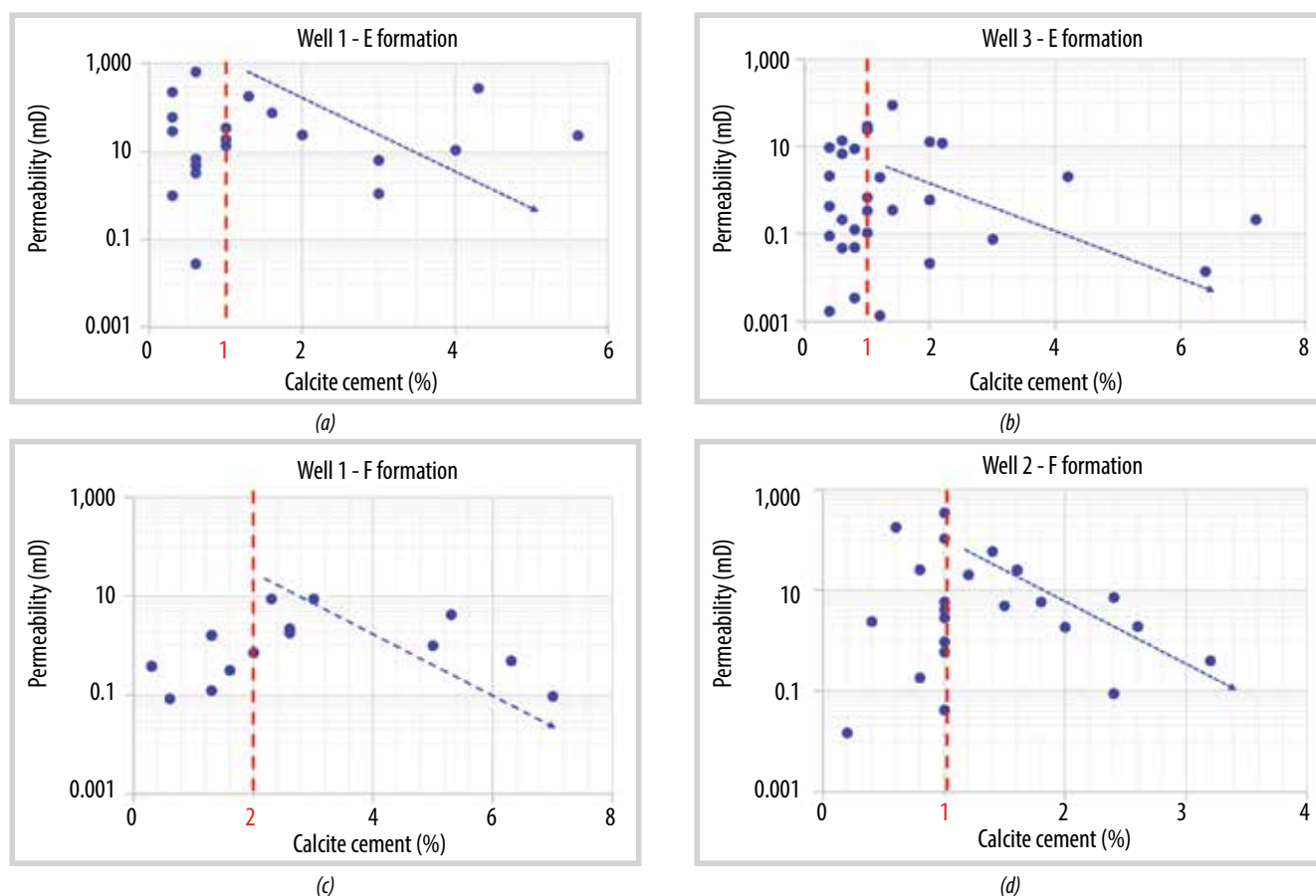


Figure 17. The relationship between permeability and calcite cements shows a negative trend.

#### 4.3.4. Authigenic clays

The presence of clays in a sandstone across all wells tends to degrade reservoir quality.

Figure 13a illustrates authigenic chlorite aggregates (Ch) occurring mostly as subhedral, thin plates that can fill pore spaces, together with illite (Il) and calcite. The macro/micropore sizes of < 20 µm encompass the remaining volumes of an occluded primary pore. A pore throat that is completely blocked by many large crystals of mosaic quartz overgrowth (q) leads to the initial pore throat not only reduced in volume but also divided into very small pore channels (arrow) and becomes very tortuous (Figure 13b).

Figure 13c suggests the remaining intergranular pores (arrows) have now become isolated or retain very poor connectivity. In addition, authigenic illite aggregates (Il) fill in the intergranular pores and pore throats, illustrating how a small amount of authigenic illite can degrade the permeability.

Authigenic chlorite clay minerals occur as thin mats of crystals that coat detrital grains. Wispy and webby illite intermixed with platy chlorite can completely coat detrital grains and fill intergranular pores, resulting in a strongly reduced permeability (Figure 13d).

Detrital feldspar grains (F) can be dissolved, forming secondary pores. The orientation of the feldspar remnants suggests that dissolution is crystallographically controlled. Locally, feldspar remnants are partly albitised and have been replaced with chlorite. This suggests that the dissolution of unstable detrital grains likely pre-dated chloritisation in the paradiagenetic sequence (Figure 13e).

Figure 13f shows a blocky authigenic zeolite crystal (Z) that occupies intergranular pore space, thus damaging the reservoir quality. A feldspar grain (F) has also been dissolved and albitised. Locally, authigenic clay minerals (Cl) occur as chlorite and illite/illite-smectite that fill in the secondary pores and can partly coat detrital grains. The strong development of quartz overgrowths (upper left) has also occluded pore throats.

Laumontite (a zeolite mineral) can replace feldspar as double-edge crystal grains or cleavage crack fills. Some pore-filling laumontites, as well as quartz overgrowths, can slow or inhibit further compaction (Figure 13c).

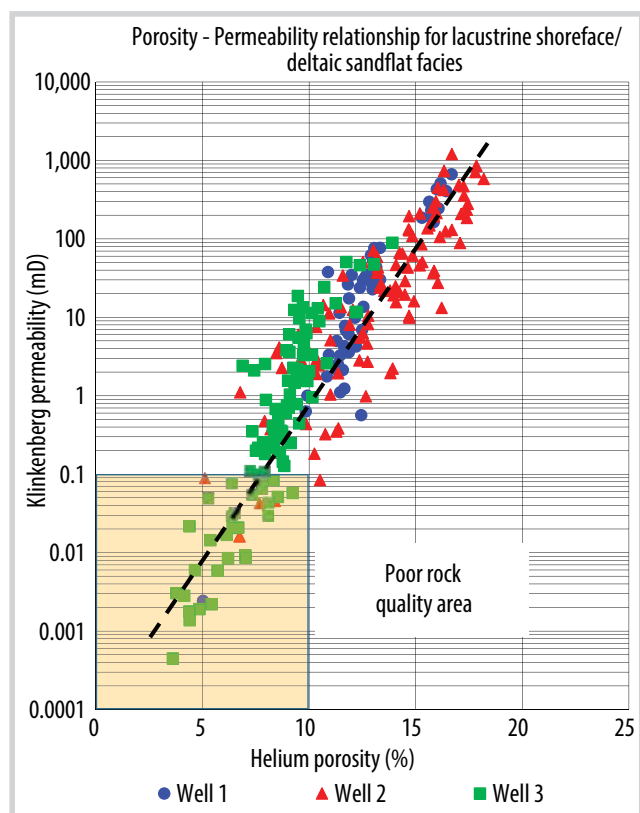
A negative relationship between total clay minerals and poroperm suggests the clay minerals are strongly de-

grading the porosity and permeability (Figures 14 and 15). Pore-lining chlorite is directly precipitated on the surfaces of grains, extending into pore space, leading to a significant decrease in permeability (Figure 13a). Illite occurs as pore-linings and is partly pore filling and partly grain coating. It forms irregular flakes with lath-like projections that can bridge intergranular spaces, thus decreasing permeability and pore throat diameters (Figures 13b and 13d). Smectite/illite transforms into illite at higher temperatures and rarely occurs in the temperature ranges of most petroleum fields unless the reservoir is flushed by hydrothermal waters.

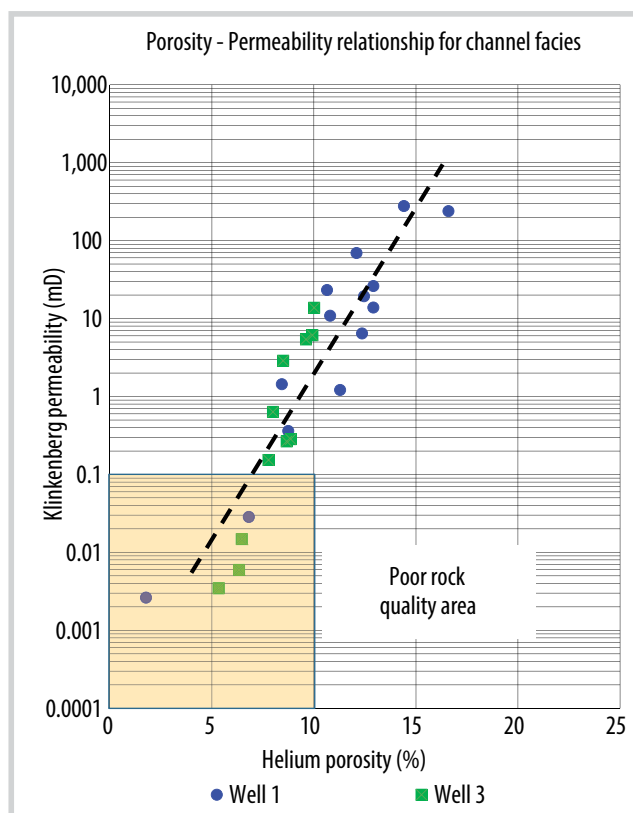
#### 4.3.5. Quartz, carbonate cements

Carbonate cements in the study area are composed of calcite with minor dolomite and siderite. Carbonate cements are observed in all wells and it is a significant factor influencing the poroperm quality of the studied sandstones. Figure 16a shows the abundance of carbonate cements is less than a certain threshold (about 10%) and illustrates the different amounts between the wells. The proportion of carbonate cements increases up to 32% in the formation E of well 1 (well\_E) and 20% in well 2 (Figure 16a) with an average of 3% of rock volume in both wells. Carbonate cements in well 3 and well 1\_F are less, with an average of 1.3% and 2.6%, respectively. Figure 17 is a cross-plot with a carbonate cement value threshold of 1% or 2%; values less than this show an unclear relationship between carbonate cement and poroperm. However, when the proportion of calcite cements is higher than 1% (well 1\_E, well 2, and well 3) or 2% (well 1\_F), there is a decrease in porosity and permeability with increasing carbonate cement content (Figure 17).

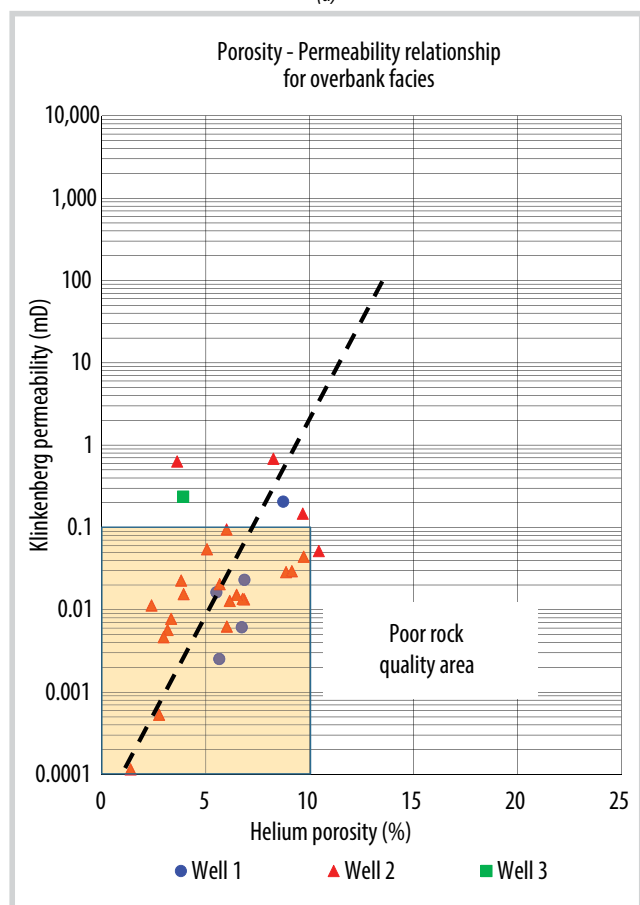
Quartz overgrowth cements, which are more abundant than carbonate cements, range from 4 % to 10%, average 7.4% in formation E of well 1, and mostly 3 - 6% (average 3.9%) in well 3, and 2.7% in well 2, which also contains the highest levels of overgrowths from 4 - 15% (average 11.8%). The formation of quartz (overgrowth) cement is an ongoing diagenetic process. It begins as one of the earlier burial phases when it can be covered by chlorite rims and can proceed until it fully fills primary pores (Figure 16b). Later quartz overgrowth cement generations develop over authigenic illite and are present as pyramidal quartz and euhedral quartz crystals that partly fill primary porosity (Figures 13b, c, d).



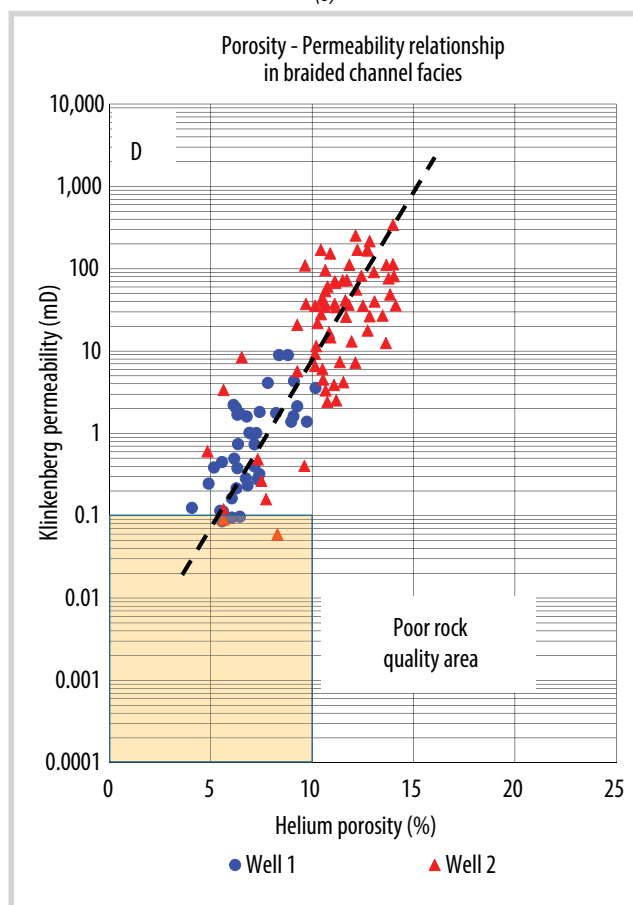
(a)



(b)



(c)



(d)

Figure 18. The poroperm relationship illustrates significant trends between facies.



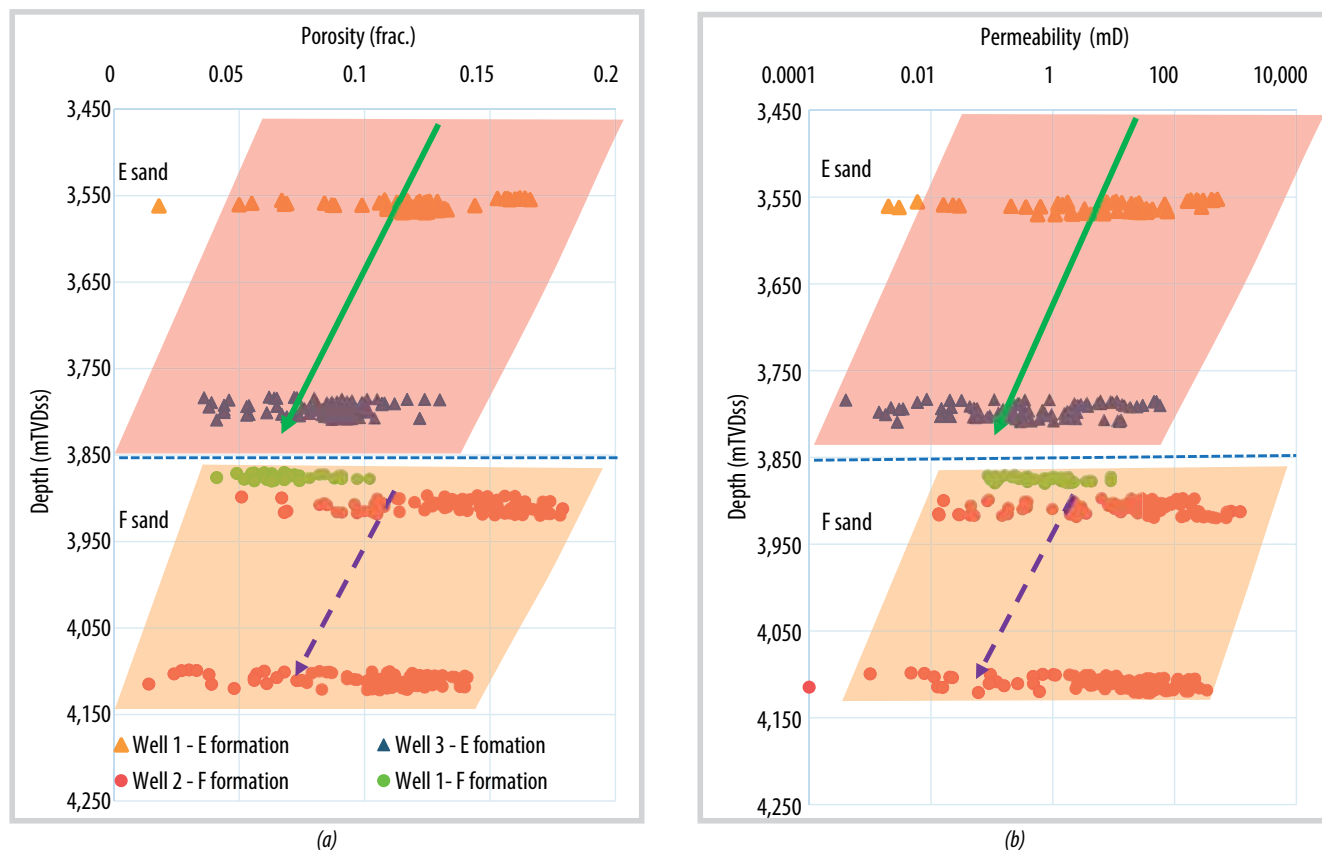


Figure 19. Core porosity (a) and core permeability, (b) vs. true vertical depth subsea cross plots.

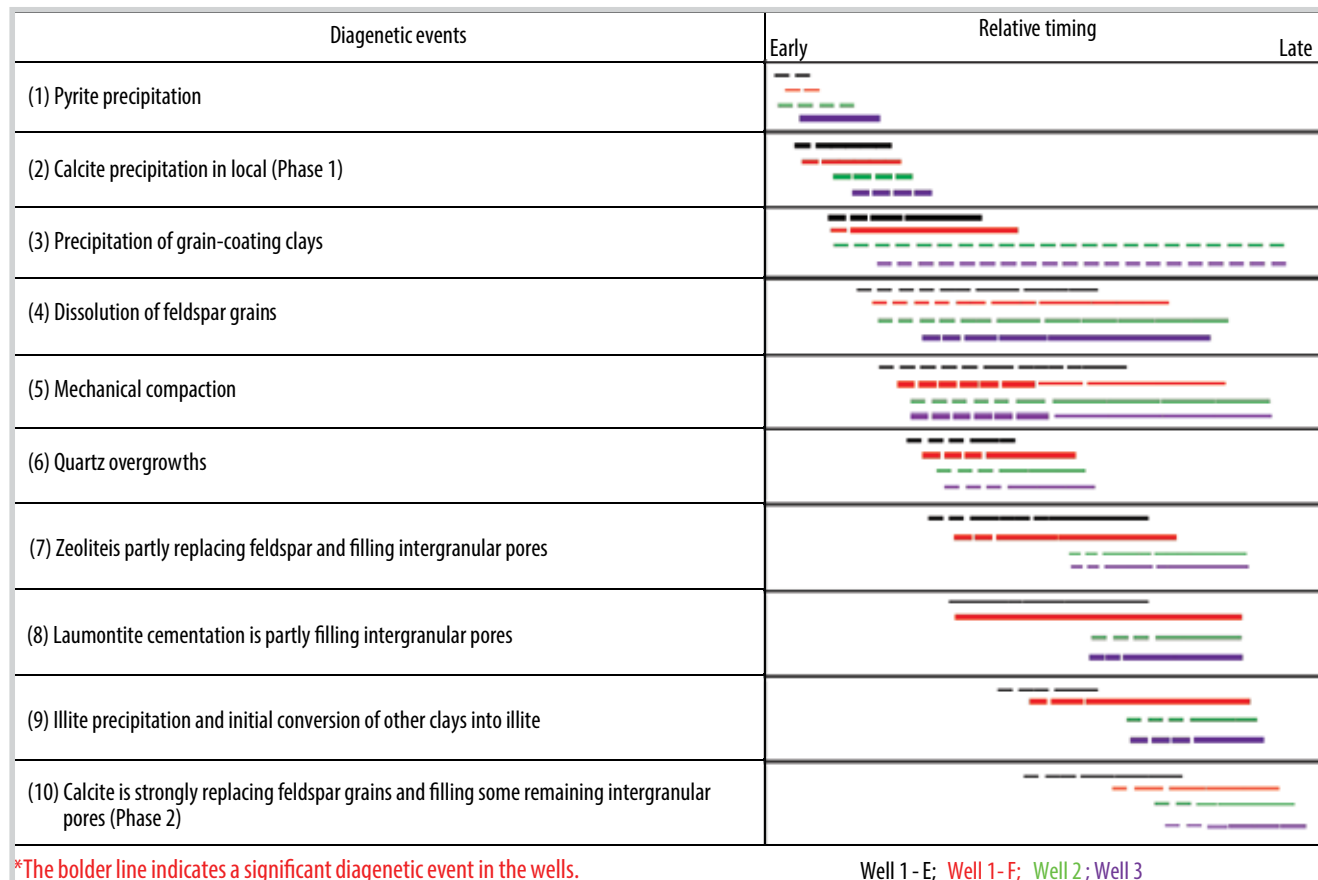


Figure 20. Paragenetic sequences across all wells.

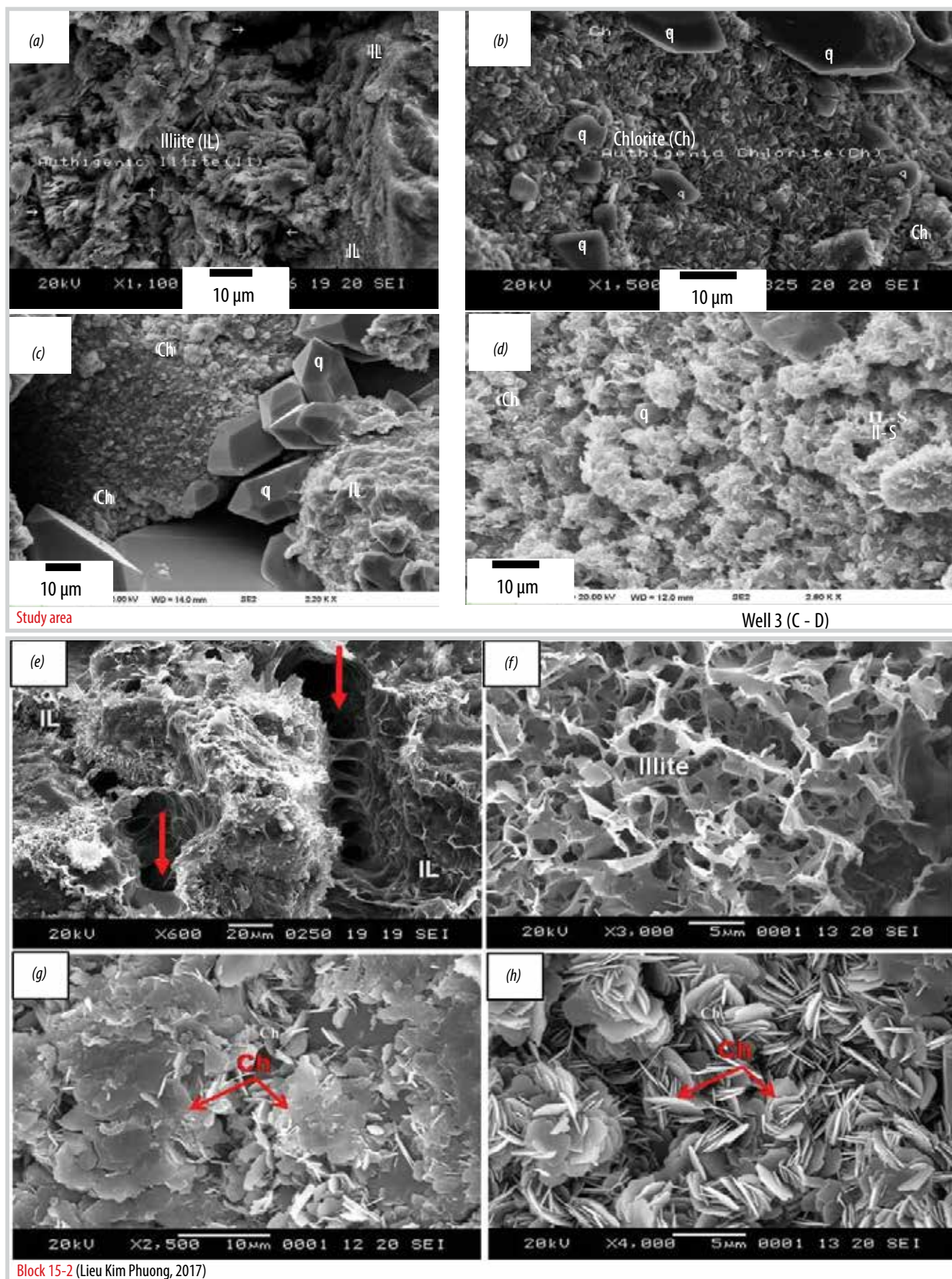


Figure 21. Morphologies of clay minerals in formation E in the study area compared to sediments in Block 15-2, Cuu Long basin [7].

## 5. Discussion

### 5.1. Key geological factors impacting porosity and permeability in sandstone reservoir

#### 5.1.1. Depositional environment

Based on the preceding observations, the lacustrine/deltaic-sandflat, channel, braided channel, and overbank deposits show significant differences in porosity and permeability. The overbank succession shows the lowest values (approximately  $\Phi_{\text{avg.}} = 5.9\%$ ,  $K_{\text{avg.}} = 0.1$  mD); moderately higher values are observed in the channel and braided channel facies (about  $\Phi_{\text{avg.}} = 9.7\%$ ,  $K_{\text{avg.}} = 28.8$  mD and  $\Phi_{\text{avg.}} = 9.5\%$ ,  $K_{\text{avg.}} = 34.9\%$ , respectively); and the highest measured values occur in lacustrine shoreface/deltaic-sandflat facies. There is a good correlation of porosity and permeability in cross-plots of these facies (Figure 18). Well 3 and well 2 show lower porosity and low permeability ( $\Phi = 10\%$ ,  $K = 0.1$  mD) observed in several samples (marked by orange box) from the otherwise good quality lacustrine/deltaic sandflat facies (Figure 18a). In addition, the average porosity of well 3 ( $\Phi_{\text{avg.}} = 8.4\%$ ) is lower than well 1 and well 2 ( $\Phi_{\text{avg.}}$  of 12.7% and 13.3%, respectively) in these facies. Similarly, a few samples from the channel facies in well 1 and well 2 illustrate low porosity and permeability (orange box) (Figure 18b). Most overbank samples show low porosity and permeability due to very fine to fine grain sizes (Figure 18c). The braided channel samples show significant differences between well 1 and well 2. The porosity of well 2 is higher than well 1 (approximately 10.9% and 7%, respectively) (Figure 18d). The differences in poroperm quality between the four facies reflect different grain-size ranges in the same depositional setting and the variable influence of diagenetic alteration.

#### 5.1.2. Compaction process

Compaction can be illustrated through plots between porosity and permeability versus depth. All show an inverse relationship with porosity decreasing with depth in a particular formation (Figures 20a and 20b). However, well 1\_F is less porous than sandstone F in the upper part of well 2 because the cementation is locally strong, especially the development of quartz (overgrowth) cement (from 11% up to 15%, Figure 16b). Petrography shows quartz is widespread as large, euhedral and syntaxial overgrowth crystals (up to 10s and 100s  $\mu\text{m}$  in length), which can completely fill the remaining intergranular pores and block pore throats in well 1\_F.

#### 5.1.3. Diagenetic process

Based on the above investigations and burial-history locations, the main diagenetic events observed in sandstones E and F are summarised in Figure 21.

Some parts of sandstones E and F show more advanced diagenetic textures such as moderate compaction, strong development of quartz and albite overgrowths, pore-filling zeolites and calcite cements. Furthermore, the dissolution of unstable detrital grains and their conversion to more stable phases are also quite common. For instance, feldspar grains are partly dissolved or replaced by laumontite, zeolite and/or calcite. This suggests that the sandstone has been transformed into hydrothermal cross-flows at moderate burial depths. Cements and authigenic minerals consist mainly of quartz overgrowths (commonly 7 - 9% in formation E and 11 - 15% in formation F), zeolites (5 - 8% and 5 - 10%, respectively) with small amounts of calcite and authigenic clays. Zeolite and calcite often form patches enclosing closely-packed detrital grains or filling in isolated intergranular pores. Remnant primary porosity was protected by the development of quartz and albite overgrowths. Grain contacts are mainly long and concavo-convex types, tending to minimise the dimensions of pore throats.

### 5.2. Comparison of diagenesis between the study area and a nearby area

The study area is located near Block 15-2 where a study was conducted on formation E [7, 8]. Their work concluded that the main factors influencing rock quality were compaction, cementation, and dissolution of unstable grains. My work concludes that the porosity and permeability in the studied wells are controlled by depositional setting variably overprinted by cementation and mechanical compaction. Authigenic clay minerals as pore-linings or in grain-surrounding coats have destructive effects on porosity and permeability. The destructive effects of increasing clay content are similar in both areas (Figures 21 a-d vs. e-f).

## 6. Conclusions

The quality of reservoir sands in the study area is evaluated by integrating all petrography, X-ray diffraction, Routine core analysis, and special core analysis data sets. The results quantify variations in the internal properties of the sandstone reservoirs. Based on the results, the conclusions of this study are:



- There are four core-defined depositional facies, namely: (i) lacustrine shoreface/deltaic sandflat (channel abandonment) sands which entrain numerous mud layers; (ii) channel sands which are generally indicated by fining-upward, bell shapes in GR and mostly found in formation E; (iii) braided channel sands which are characterised by poorer sorting with mostly blocky shapes in GR, and mostly abundant in the formation F; (iv) the overbank succession which shows the lowest poroperm values. Moderately higher poroperm values are observed in the channel and braided channel facies and the highest values tend to occur in lacustrine shoreface/deltaic-sandflat (channel abandonment) facies.

- Rock property measures across the E and F formations show porosity and permeability values ranging from low to high. Generally, there is a tie to the depositional setting. But in the intervals that are more affected by diagenesis and hydrothermal fluid crossflows, the enhanced formation of authigenic cements can degrade what were good quality sands at the time of deposition.

- The curvature of capillary pressure curves indicates the rock quality. Some samples show a gentle curvature that relates to reduced permeability, poorer sorting, finer grain sizes and the impact of calcite cements.

- Thin-section study shows that rock quality was significantly controlled by a combination of mechanical and chemical compaction, as shown by grain contacts ranging from point-to-point to long-axis rotation, and concavo-convex styles being present in all three wells.

- The negative relationship between total clay minerals and poroperm suggests that clay minerals reduce porosity and permeability. Pore-lining chlorite is directly precipitated onto detrital surfaces of grains and extends into pore space, leading to decreasing permeability. Authigenic illite also decreases permeability by blocking pore throats.

- Chlorite is more abundant in sandstone E than in the sandstone F. Chlorite tends to develop in the sandstones which are richer in volcanic fragments. By contrast, illite is present in the sandstone F at much higher levels than in the sandstone E, thus, illite is likely a weathering product, but diagenetic illite is also created by reactions of smectite with pore fluids during deep burial.

- Calcite cements can fill pores, reducing permeability and porosity in all wells. It can show a patchy

or uneven distribution and was mostly generated in early diagenesis.

- Compaction is illustrated in plots of porosity and permeability with depth. These plots show an inverse relationship with poroperm decreasing with depth.

- Sandstones E and F have experienced a complex diagenetic evolution as follows: (1) (2) pyrite and calcite precipitation, (3) precipitation of grain-coating clays, (4) dissolution of feldspar grains, (5) mechanical compaction, (6) quartz overgrowths, (7) zeolites partly replacing feldspars, (8) laumontite cementation, (9) illite precipitation, (10) calcite strongly replacing feldspar grains.

- A comparison with a result from a nearby area shows the depositional rock quality of formation E in that area was similarly influenced by diagenetic processes, such as compaction, cementation, and dissolution. The study in the adjacent area concludes that porosity and permeability were greatly impacted by the formation of authigenic clays, such as chlorite or illite, as well as mechanical compaction.

### Acknowledgements

I am very grateful to my supervisor, Prof. John Keith Warren, who continually and convincingly conveyed a spirit of challenge throughout my research.

I would also like to thank the Exploration and Production Centre of the Vietnam Petroleum Institute and the Vietnam National Oil and Gas Group for providing the dataset for this research.

### References

[1] Robert J. Morley, Bui Viet Dung, Nguyen Thanh Tung, A.J. Kullman, Robert T. Bird, Nguyen Van Kieu, and Nguyen Hoai Chung, "High-resolution Palaeogene sequence stratigraphic framework for the Cuu Long basin, offshore Vietnam, driven by climate change and tectonics, established from sequence biostratigraphy", *Palaeogeography, Palaeoclimatology, Palaeoecology*, Vol. 530, pp. 113-135, 2019. DOI: 10.1016/j.palaeo.2019.05.010.

[2] Nguyen Xuan Huy, Bae Wisup, Ngo Thuong San, V.T. Xuan, J. Sung Min, and Kim D.Y., "Fractured basement reservoir and oil displacement mechanism in White Tiger field, offshore Vietnam", *AAPG Search and Discovery Article, Singapore*, 16 - 19 September 2012.

[3] Tran Le Dong and Phung Dac Hai, "Cuu Long

sedimentary basin and petroleum resources”, *The petroleum geology and resources of Vietnam*, Science and Technics Publishing House, 2007.

[4] William Jay Schmidt, Bui Huy Hoang, James W. Handschy, Vu Trong Hai, Trinh Xuan Cuong, and Nguyen Thanh Tung, “Tectonic evolution and regional setting of the Cuu Long Basin, Vietnam”, *Tectonophysics*, Vol. 757, pp. 36 - 57, 2019. DOI:10.1016/j.tecto.2019.03.001.

[5] “High resolution biostratigraphy report well 1, Block X, Cuu Long basin”. 1974.

[6] Robert L. Folk, *Petrology of sedimentary rocks*. Hemphill Diesel Eng Schools, 1974.

[7] Lieu Kim Phuong, Le Thi Thu Hang, Nguyen Van Hieu, and Nguyen Minh Nhut, “Characterization

of petrography and diagenetic processes influence on porosity and permeability of Oligocene sandstone reservoir rocks, Block 15-2 in Cuu Long basin”, *International Journal of Engineering Research and Applications*, Vol. 7, No. 6, pp. 62 - 73, 2017. DOI:10.9790/9622-0706076273.

[8] Ho Minh Toan, Lieu Kim Phuong, Doan Thi Thuy, and Bui Thi Ngoc Phuong, “Generation of authigenic clay minerals during diagenesis and their influences on porosity and permeability of Oligocene sandstones reservoir rocks, from a well in the west of Cuu Long basin”, *Science & Technology Development Journal*, Vol. 17, No. 3, pp. 21 - 26, 2014. DOI: 10.32508/stdj.v17i3.1456.